Modern Assessment of Natural Hydrocarbon Gas Flux at the Coal Oil Point Seep Field, Santa Barbara, California

A. M. Padilla[1], S. Loranger[1], F. S. Kinnaman[2], D. L. Valentine[2] and T. C. Weber[1]

[1]Center for Coastal and Ocean Mapping, University of New Hampshire, Durham, NH.

[2]Department of Earth Science and Marine Science Institute, University of California, Santa Barbara, CA.

Corresponding author: Alexandra M. Padilla (apadilla@ccom.unh.edu)

Key Points:

- Acoustic estimates of shallow, natural hydrocarbon gas flow
- Direct *in situ* measurements of shallow, natural hydrocarbon gas flux
- Coal Oil Point natural hydrocarbon seep field

Abstract

The Coal Oil Point seep field is among the most active and studied hydrocarbon seep fields in the world. The water column of the Coal Oil Point seep field was acoustically surveyed from 31 August 2016 to 14 September 2016 with a 200 kHz split-beam echosounder to map the distribution of natural hydrocarbons in the region. An *in situ* direct capture device was used to measure the volumetric gas flux of natural hydrocarbons for three localized seep sites while simultaneously collecting acoustic volume backscatter measurements of the hydrocarbons within the water column. The acoustic volume backscatter was calibrated with the measured volumetric gas flux and the resulting relationship was used to determine flux over the entire seep field. The estimate of integrated volumetric gas flow rate over a survey area of approximately 4.1 km^2 was 23,800 m^3/day. The estimates of integrated volumetric gas flow rate and volumetric gas flux were compared to measurements reported in previous studies and were two to seven times smaller than results obtained by Hornafius et al., (1999), which had a total survey area of 18 km^2. However, differences between methodologies limit the ability to assess natural variability in the Coal Oil Point seep field.

Plain Language Summary

Coal Oil Point is one of the largest and most studied natural underwater hydrocarbon seep sites in the world. Coal Oil Point is located within the Santa Barbara Channel off California's coast and researchers have been studying this natural hydrocarbon site for five decades to understand how the release of petroleum from the seafloor affects the ocean, atmosphere and living organisms. This study combines acoustic measurements from a broad scale survey, with direct observations of gas flow rates, in order to map the contemporary distribution of seeps and obtain estimates of total gas flow rate for the study site. The total gas flow rate for the surveyed area, a total area of 4.1 km^2, was approximately 23,800 m^3/day. The gas flow rates from this study were compared to estimates reported in previous studies and showed that current gas flow rates range from two to seven times lower than those reported in 1999 (total survey area of 18 km^2). However, due to differences in the approaches used to estimate the gas flow rate in the region, it is difficult to address if the change in gas flow rates is caused by natural variability or due to differences in methodology between studies.

1 Introduction

Natural hydrocarbon seeps occur along continental shelves and in the deep ocean, releasing hydrocarbons as gas bubbles, dissolved gas and/or oil droplets into the water column from the seafloor. The Santa Barbara Channel, located on the Southern California coast, is one of the most active and persistent natural hydrocarbon seep fields in the world (Hovland and Judd, 1992; Hill et al., 2006) and has been emitting hydrocarbons for tens to hundreds of thousands of years (Boles et al., 2004; Hill et al., 2006; Valentine et al., 2010). Coal Oil Point, a seep field located in the Santa Barbara Channel off the south coast of Goleta, California, has been deemed, "one of the most prolific natural hydrocarbon seepage sites in the world" (Hornafius et al., 1999; Quigley et al., 1999). Gas bubbles and oil droplets released within this seep field can be visually observed rising to the surface of the water column and previous research suggests that methane released from shallow depths (<100 m) facilitates the transport of methane into the atmosphere (Clark et al., 2003; Clark et al., 2010; Leifer et al., 2000; Mau et al., 2007).

During the years 1994 and 1995, Hornafius et al. (1999) conducted a broad scale acoustic survey to map the distribution of natural hydrocarbon seepage activity and estimate the volumetric gas flow rate in the region. Their estimate of volumetric gas flow rate for the Coal Oil Point seep field, over an area of 18 km^2, was approximately 1.48 x 10^5 m^3/day (Hornafius et al., 1999). More recent studies have been conducted in order to map the present distribution of natural hydrocarbons in the Coal Oil Point seep field (Leifer et al., 2010) and obtain localized estimates of volumetric gas flow rates within the region (Clark et al., 2010; Washburn et al., 2005). However, since the study conducted by Hornafius et al. (1999), no volumetric gas flow rate estimates for the overall Coal Oil Point seep field, using acoustic techniques, have been reported. The goal of this study is to map the present spatial distribution of natural hydrocarbon seeps within the Coal Oil Point seep field and estimate the volumetric gas flow rate within the surveyed region.

Previous studies have exploited acoustic techniques to observe and map natural hydrocarbon seeps in Coal Oil Point and other ocean basins (Greinert el al., 2006; Heeschen et al., 2003; Hornafius et al., 1999; Leifer et al., 2010; Quigley et al., 1999; Römer et al., 2017; Weber et al., 2014). The acoustic volume backscattering strength, S_v, which is the decibel equivalent of the volume backscatter coefficient in a unit volume, has been used previously to estimate gas and oil flux emissions (Nikolovska et al., 2008; Weber et al., 2012). One of the drawbacks of these acoustic approaches is that without prior knowledge of the nature of the seep, such as bubble size distribution, relative number of gas bubbles and oil droplets in the water column and the physical properties of the gas and oil present in the seep (Loranger et al., 2018), it is difficult to perform a complete acoustic inversion to estimate gas/oil flux. Broadband acoustic methods have been used to help overcome this problem in the past (Medwin and Breitz, 1989; Terrill and Melville, 2000; Vagle and Farmer, 1992), but direct sampling is also used to help calibrate the acoustic results (Greinert et al., 2010; Nikolovska et al., 2008; Römer et al., 2012a; Römer et al., 2012b; Wang et al., 2016; Weber et al., 2014).

In this study an acoustic survey of the Coal Oil Point seep field was conducted in order to map the seep distribution and quantify the relative acoustic gas flow in the region. *In situ*, direct capture measurements of volumetric gas flux were collected simultaneously within a subset of the acoustic backscatter measurements to establish a relationship between the acoustic volume backscatter coefficient and volumetric gas flux. This relationship was used to calibrate the acoustic survey results to provide an integrated measurement of volumetric gas flow rate from the region and compare it to previous estimates of volumetric gas flow rates in Coal Oil Point reported in literature.

2 Acoustic Survey

Acoustic backscatter data was collected between 31 August 2016 and 14 September 2016 using a downward looking Simrad ES200-7C split-beam echosounder that was mounted on a tow sled and deployed from the port side of the *R/V Connell*. The transducer was interfaced with a Simrad EK80 Wide Band Transceiver used to transmit and receive acoustic signals. A 2 ms linear-frequency modulated transmit pulse, with a bandwidth of 150-250 kHz, was used throughout the study. The acoustic system was calibrated for transducer beam-pattern effects by following the standard–target calibration procedure described in Demer et al. (2015). Real-time positioning of the acoustic data was implemented with a Wide Area Augmentation System enabled GPS that

was attached to the tow sled. CTD casts were performed each survey day to acquire vertical profiles of sound speed and sound absorption in the water column.

The acoustic survey (Figure 1) included five focus seep sites commonly known as Platform Holly (b), Seep Tent (c), La Goleta (d), Patch (e) and Trilogy (f). With the exception of Trilogy, surveys at the focus seep sites were conducted with 10 m line spacing in a 500 m by 500 m region in water depths that ranged from 60-70 m. At Trilogy, the survey was conducted with 20 m line spacing in a 1000 m by 600 m area with water depths that ranged from 35-50 m. A broader survey consisting of six NW-SE lines and four orthogonal NE-SW lines was conducted, linking the four deeper focus seep sites.

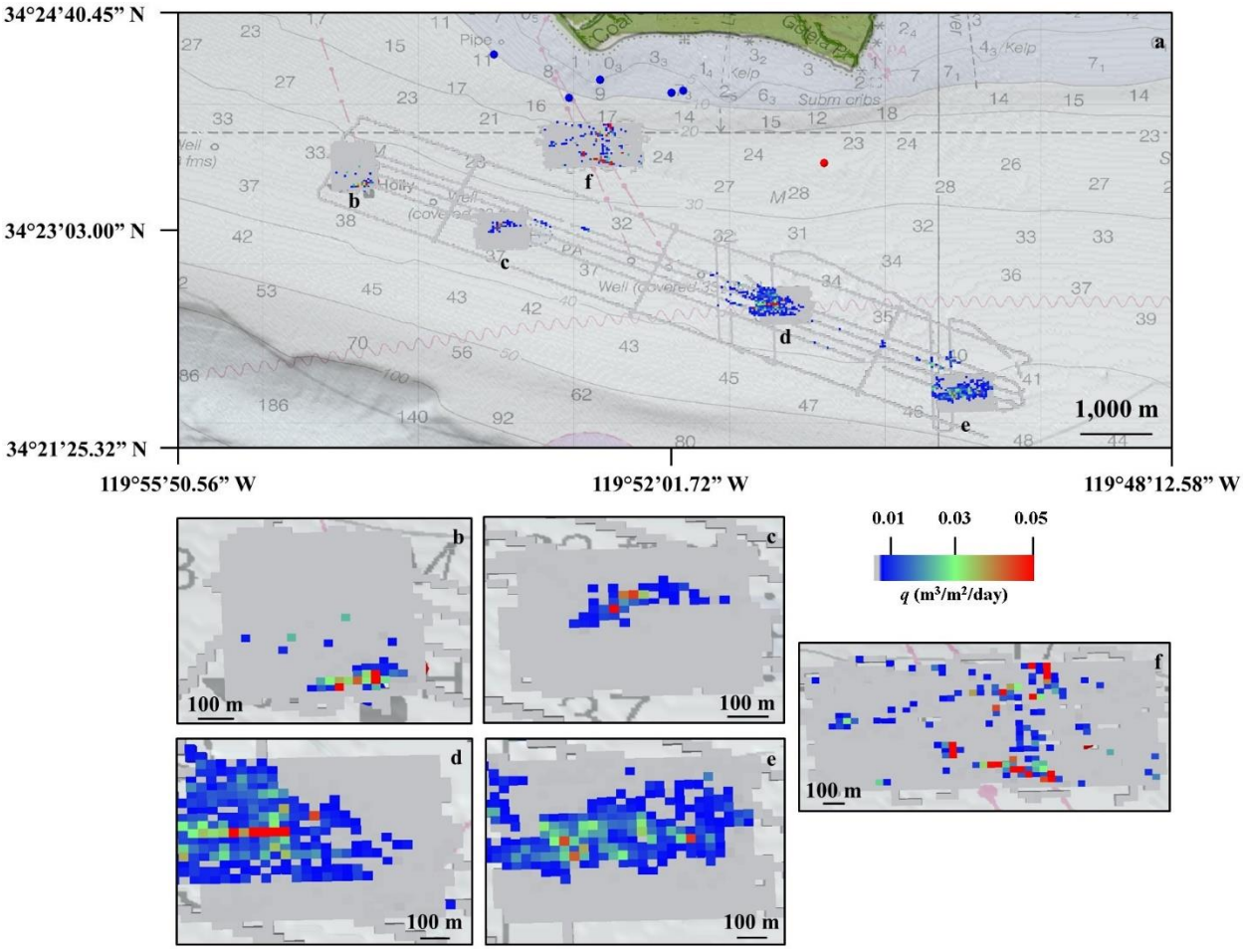

Figure 1. Estimates of 25 m by 25 m gridded volumetric gas flux ($m^3/m^2/day$) using extracted average acoustic volume backscatter coefficients (m^{-1}) from a 1 m layer at a depth of 23 m, a total pressure of approximately 326 kPa, and temperatures ranging from 13-17℃ for the entire acoustic survey. a) Volumetric gas flux heat map of the entire Coal Oil Point 2016 acoustic survey with a total volumetric gas flow rate of 23,800 m^3/day over a survey area of approximately 4.1 km^2: b) Platform Holly (6.3%), c) Seep Tent (4.2%), d) La Goleta (22.5%), e) Patch (17.7%) and f) Trilogy (37.7%); where the percentage is representative of the portion of volumetric gas flow rate at that site with respect to the total volumetric gas flow rate estimated for the entire survey. Colder colors represent areas of low volumetric gas flux, warmer colors represent areas of high volumetric gas

120 flux and gray colors represent values of volumetric gas flux that are below a 0.003 $m^3/m^2/day$
121 threshold. The red and blue dots shown in panel "a" above Trilogy are locations of other seeps in
122 the Coal Oil Point seep field.

123 Raw acoustic backscatter data were processed to obtain measurements of the volume backscatter
124 coefficient, s_v (m^{-1}). MacLennan et al. (2002) defines s_v as

125 $$s_V = \frac{\sum_{i=1}^{N} \sigma_{bs,i}}{V}, \quad (1)$$

126 where $\sigma_{bs,i}$ is the backscattering cross-section (m^2) of a single target and N is the total number of
127 targets in the ensonified volume, V. The ensonified volume is generally a function of range and
128 frequency, and is governed by the width of the echosounder beam and the range extent
129 associated with the summation in equation 1:

130 $$V = \frac{c\tau\pi\left[r\tan\left(\theta_{2,eq}\right)\right]^2}{2}, \quad (2)$$

131 where c is the speed of sound of the surrounding medium, r is the range to the measurement and
132 $\theta_{2,eq}$ is the two-way equivalent beam width of the transducer (5° for the Simrad ES200-7C split-
133 beam echosounder used throughout the study). For narrowband systems analyzed in the time-
134 domain, T is the pulse length. In this study, however, the raw acoustic data were analyzed in the
135 frequency domain using Fourier transforms, following the approach for extended targets
136 described by Weber and Ward (2015), in which case T is defined as the length of the analysis
137 window used to compute the Fourier transform (i.e., the number of samples used in the Fourier
138 transform divided by the sample rate).

139 Weber and Ward (2015) showed that for a match filtered acoustic signal, σ_{bs}, the backscattering
140 cross-section of an individual target, is defined as

141 $$\sigma_{bs}(f) = \frac{|S_{mf}(f)|^2}{C_{mf}(f)} \frac{r^4}{\exp(-4ar)}, \quad (3)$$

142 where $S_{mf}(f)$ and $C_{mf}(f)$ are the Fourier transforms of the match filtered receive signal and
143 calibration factor, respectively. The second fraction represents the two-way transmission loss due
144 to spherical spreading and absorption where r is the range in meters and a is the absorption
145 coefficient measured in nepers per meter. The absorption coefficient used here accounts only for
146 absorption in seawater (Francois and Garrison, 1982), which is on the order of 1 dB at the short
147 ranges used here and does not include the increased (and variable) attenuation due to bubble
148 scattering (Clay and Medwin, 1977). Equation 3 is for the special case where there is a single
149 target (N=1) in an ensonified volume. For the more general case when there are multiple targets
150 within a volume (N>1), the left-hand side of equation 3 becomes the sum of the backscattering
151 cross-section of the individual targets (Clay and Medwin, 1977) and can be written as

152 $$\sum_{i=1}^{N} \sigma_{bs,i}(f) = \frac{|S_{mf}(f)|^2}{C_{mf}(f)} \frac{r^4}{\exp(-4ar)}. \quad (4)$$

153 Combining equations 1, 2 and 4, s_v for a match filtered signal in the frequency domain is

$$s_v(f) = \frac{|S_{mf}(f)|^2}{C_{mf}(f)} \frac{r^4}{\exp(-4ar)} \frac{2}{cT\pi\left[r\tan(\theta_{2,eq})\right]^2}. \quad (5)$$

Equation 5 describes the processing steps used in this study: the receive signal (i.e., raw acoustic data) was match filtered and a Fourier transform over the range extent of interest was taken to generate $S_{mf}(f)$, and the result was adjusted for calibration, transmission loss, and the ensonified volume.

Acoustic backscatter data was collected throughout the entire water column, however only data within a 1 m depth layer centered at a depth of 23 m was analyzed from each ping to obtain values for s_v. This depth layer was chosen to enable the comparison of volumetric gas flow rate estimates with Hornafius et al. (1999) who reported volumetric gas flow rates at the same average depth. Estimates of s_v calculated using equation 5 were averaged over a narrow frequency band of 192-201 kHz, which was chosen due to the overlap of valid estimates of $C_{mf}(f)$ from the acoustic calibration procedure, caused by using different calibration spheres for the 2016 broad acoustic survey and the 2017 acoustic backscatter data collected in tandem with *in situ* direct volumetric gas flux measurements. The resulting s_v estimates were then averaged in 25 m by 25 m grid cells throughout the surveyed area.

The contribution of oil droplets to the estimate of s_v is assumed negligible. Gas bubbles are significantly stronger acoustic scatterers than oil droplets due to their higher acoustic impedance contrast with the surrounding seawater (Figure 2). For the oil droplets to have a non-negligible contribution to the integrated acoustic survey results, they would have to be present in far greater number than the surrounding gas bubbles, a scenario that was discounted through visual observations of surfacing gas bubbles and oil droplets during the survey.

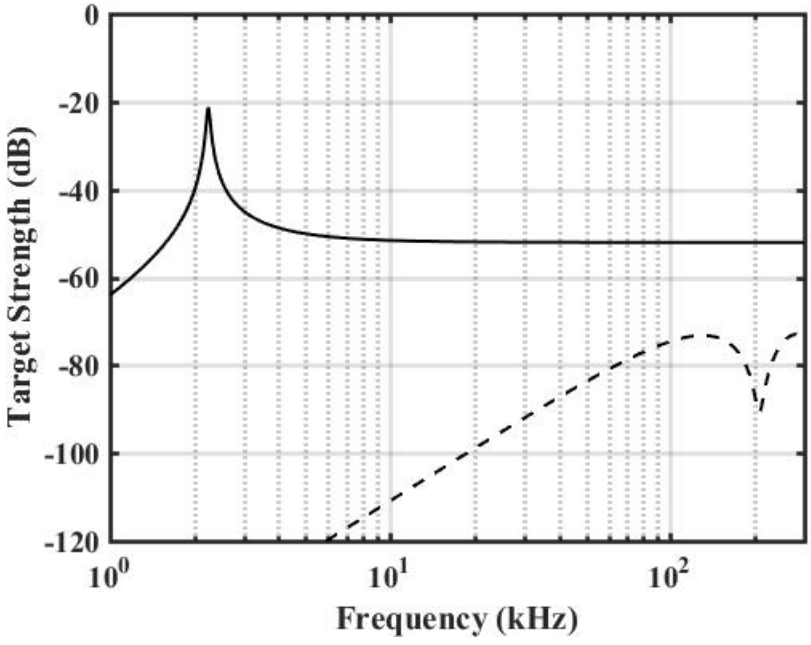

Figure 2. Frequency dependent acoustic scattering of a 2.5 mm methane bubble (solid line), using an acoustic scattering model for bubbles from Clay and Medwin (1977) and a 2.5 mm oil droplet (dashed line), using Anderson's (1950) derivation for acoustic scattering from fluid spheres.

3 Conversion of Acoustic Data to Volumetric Gas Flux

In previous studies at the Coal Oil Point seep field (Hornafius et al., 1999; Quigley et al., 1999) acoustic backscatter measurements were converted to volumetric gas flux using synthetic plumes, where a synthetic plume is an artificial source of gas in the water column. Acoustic measurements were made over a synthetic plume with the assumption that both the synthetic plume and the natural seep have the same bubble size distribution. There is some inherent bias in this approach due to potential and unknown differences in the bubble size distribution between the synthetic plume and the natural seep. For example, the s_v over a frequency range of 50-250 kHz, of twenty-five 1 mm radius bubbles is equivalent to the s_v of a single 5 mm radius bubble, however the volume of gas transported by the single 5 mm radius bubble is five times greater than the volume of gas transported by the twenty-five 1 mm radius bubbles. In this study however, the natural plumes in the seep field were used rather than a synthetic plume to convert the acoustic backscatter measurements to estimates of volumetric gas flux and avoid potential bias in assuming that a synthetic plume and natural plume have the same bubble size distribution. A bubble catch device (BCD, shown in Figure 3) similar in concept to the "Flux Buoy" developed by Washburn et al. (2001), was constructed to calibrate the acoustic backscatter data for volumetric gas flux. The BCD performed a timed direct capture of the gas into a known volume and was collected simultaneously with acoustic backscatter data in order to establish a relationship between s_v and volumetric gas flux.

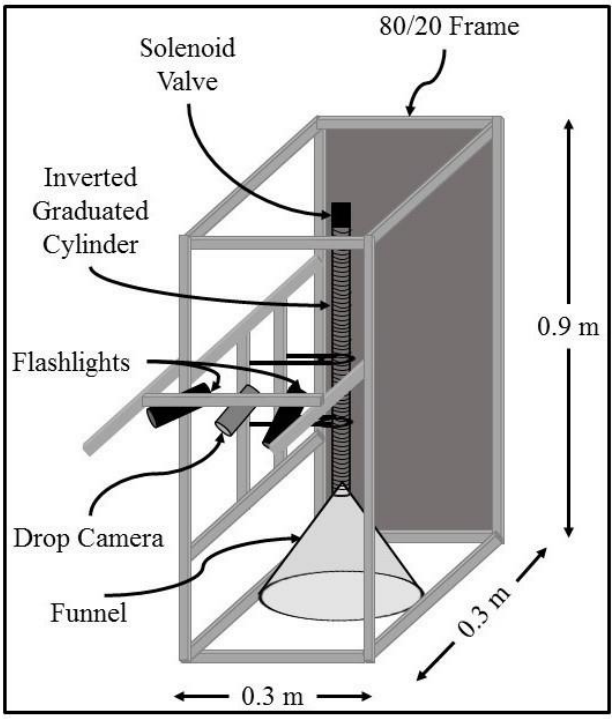

Figure 3. Bubble catch device (BCD) schematic.

The BCD was constructed by attaching an inverted graduated cylinder to an aluminum frame. Bubbles were guided into the inverted graduated cylinder through a high-density polyethylene funnel, located at the base of the frame that had a cross-sectional area of approximately 0.085 m^2. An underwater camera was mounted to the BCD and used to monitor and record the height of the gas-water interface within the graduated cylinder. Once the graduated cylinder was filled with gas, the gas was released via a surface-controlled solenoid valve attached to the top of the graduated cylinder. This configuration facilitated continuous and replicate volumetric gas flux measurements with the BCD without having to recover the instrument.

On 26 October 2017, the BCD and a 200 kHz split-beam echosounder were deployed to collect *in situ* volumetric gas flux measurements and acoustic backscatter data at three of the focus seep sites in the Coal Oil Point seep field: Platform Holly, Seep Tent and La Goleta. The echosounder was pole-mounted on the port side of the *R/V Connell* while the BCD was hand deployed from the starboard side. The echosounder was the same one used to obtain acoustic backscatter measurements during the 2016 broad acoustic survey and was also calibrated using the standard-target calibration procedure described in Demer et al. (2015). The BCD was deployed to a depth of 23 m at Seep Tent and La Goleta and to 15 m at Platform Holly. The BCD was deployed at a shallower depth at Platform Holly to avoid potential contact with the platform subsea structure. The *R/V Connell* was positioned at locations of high seep activity, determined acoustically at each seep site. The vessel then drifted over the seep until no volumetric gas flux activity was evident in the video and acoustic data. The BCD was then recovered, and the vessel returned to a location of high seepage activity to repeat the process at each seep site. A total of 17 independent time series' of *in situ* direct volumetric gas flux measurements and s_v were collected at the three seep sites: five at Platform Holly, four at Seep Tent and eight at La Goleta.

The rate of accumulation of gas was measured by tracking the meniscus of the gas-water interface within the graduated cylinder from the images collected with the BCD. The meniscus height of the gas-water interface was sampled at two frames per second and smoothed with a running average filter (Figure 4-a). The vertical volumetric gas flux, q ($m^3/m^2/s$), through the funnel base was estimated using

$$q(t)=\frac{\frac{dh(t)}{dt}A_{cylinder}}{A_{funnel}}, \quad (6)$$

where $\frac{dh(t)}{dt}$ is the rate of accumulation of gas within the graduated cylinder (m/s) and $A_{cylinder}$ and A_{funnel} are the cross-sectional areas (m^2) of the graduated cylinder and the funnel base, respectively.

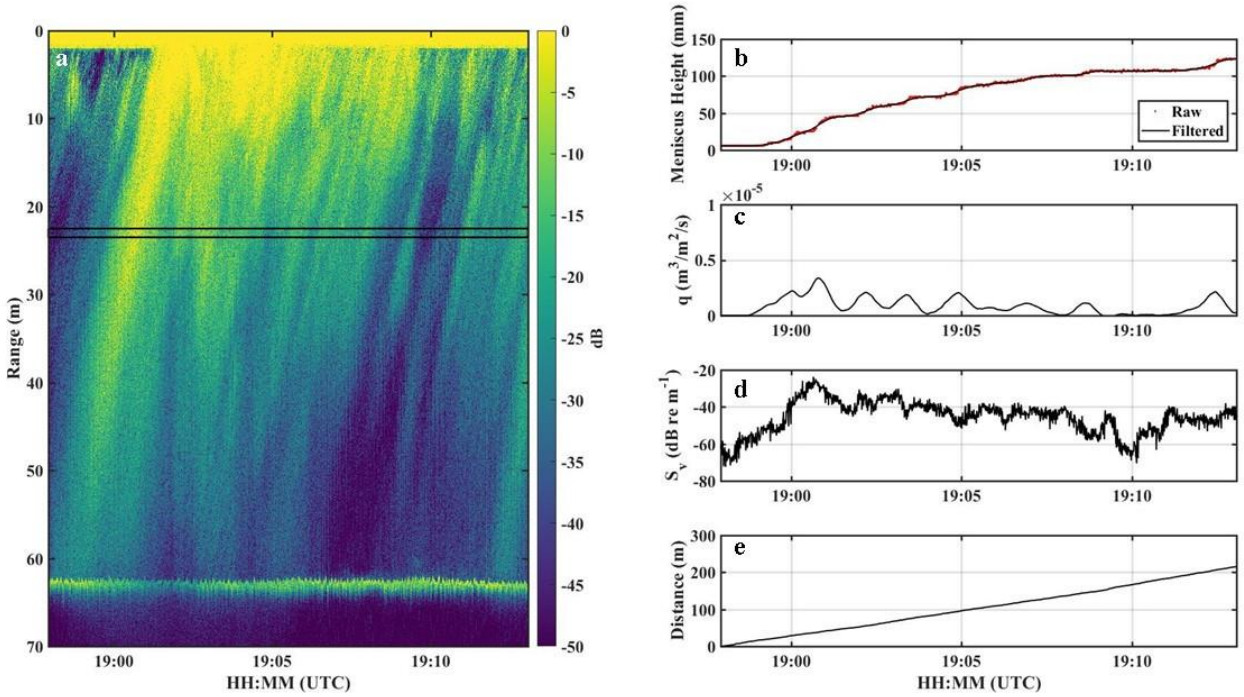

Figure 4. An example of *in situ* volumetric gas flux and acoustic backscattering observations collected at La Goleta (26 October 2017). a) Raw match filtered echogram. The black box represents the 1 m layer of data extracted to calculate s_v at a depth of 23 m. b) Measured meniscus height (mm). c) Estimated volumetric gas flux ($m^3/m^2/s$) from video images. d) Volume backscattering strength (dB re m^{-1}). e) Cumulative distance (m) traveled over the sample period.

Although *in situ* volumetric gas flux and acoustic backscatter measurements were obtained simultaneously, they did not sample the same portion of the water column. The instruments were separated by the width of the vessel (approximately 3 m). At the BCD deployment depths, 15 m and 23 m, the radius of the ensonified area of the echosounder (nominal one-way beam width of 7°) is 0.92 m and 1.4 m, respectively. The minimum horizontal distance between the sample volumes of the instruments is approximately 2.6 m. The intensity of seeps can vary up to 20-25 dB and 0.25 m^3/m^2/day over distances of the same order of magnitude as the separation of the instruments (Figure 4). In order to address the fact that both instruments were sampling different volumes within the water column, the *in situ* volumetric gas flux measurements and s_v estimates were time averaged for each independent time series measurement. The underlying assumption behind averaging the independent time series is that as the vessel drifts over great distances, the BCD and echosounder will, on average, capture the same sample volume of volumetric gas flux and acoustic backscatter. The relationship between the time averaged volumetric gas flux measurements and the time averaged s_v estimates are shown in Figure 5. Observations (N=2) where the cumulative distance traveled (4 m and 13 m), during the measurement collection, was of the same order of magnitude as the separation between the instruments (the circled points in Figure 5) were considered outliers and excluded from further analysis.

The correlation between s_v and volumetric gas flux can be obtained by understanding how the average acoustic backscattering cross-section of an ensemble of bubbles within a sample volume

(s_v) varies as a function of the void fraction of bubbles (β) within the same sample volume. s_v is estimated mathematically as

$$s_v = \frac{N \int \sigma_{bs}(R)\rho(R)dR}{V}, \quad (7)$$

where R is the bubble radius, N is the total number of bubbles within the sample volume, $\rho(R)$ (m^{-1}) is the probability density function of the bubble size distribution, V is the sample volume and $\sigma_{bs}(R)$ is the backscattering cross-section of a bubble. Equation 7 is valid under the assumption that multiple scattering between bubbles is negligible. The void fraction of bubbles within a sample is defined as

$$\beta = N \frac{\int \frac{4}{3}\pi R^3 \rho(R)dR}{V}. \quad (8)$$

If $\rho(R)$ is assumed to be unchanging, as is the case in this study, then the integrals in equations 7 and 8 are constants. Therefore, if the number of bubbles in β increases (i.e., the total number of bubbles, N, increases within a sample volume), s_v increases linearly and vice versa. Accordingly, a linear regression was fitted to the remaining data (N=15; mean cumulative distance of 60 m with a range of 16-215 m) to correlate s_v to volumetric gas flux and found to have a r-squared and p-value of 0.75 and 2.7 x 10^{-5}, respectively.

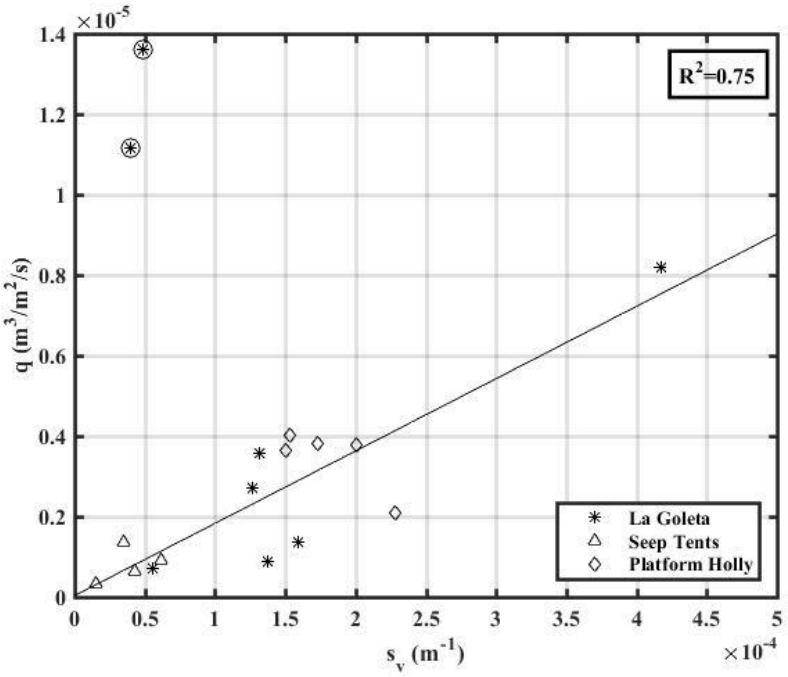

Figure 5. Time average volumetric gas flux from the BCD versus the time average s_v from 17 independent measurements obtained on 26 October 2017. The circles surrounding the data points for La Goleta represent outlier data points and they were not used to correlate volumetric gas flux estimated from the BCD to the acoustic estimates of s_v, as described in the text. The solid line is the linear regression between s_v and volumetric gas flux.

The correlation between s_v and volumetric gas flux was used to convert gridded s_v measurements to volumetric gas flux in units of $m^3/m^2/day$ (Figure 1) at a total pressure of approximately 326 kPa and temperatures ranging from 13-17 °C. A threshold volumetric gas flux value (0.003 $m^3/m^2/day$) was determined by calculating the mean estimate plus three standard deviations of s_v for areas that contained no acoustic evidence of gas bubbles within the water column and converting the acoustic threshold to volumetric gas flux. The volumetric gas flow rate, Q (m^3/day), for each focus seep site was obtained by discarding volumetric gas flux values below the determined threshold, converting estimates of volumetric gas flux at depth to volumetric gas flux at standard temperature and pressure (STP, 0 °C and 101 kPa), to account for volume expansion, and integrating the remaining gridded volumetric gas flux estimates in the region (Table 1). Estimates of volumetric gas flux were reported at STP for comparison with previous studies. The total volumetric gas flow rate for the 2016 survey, over a total surveyed area of 4.1 km^2, at STP is approximately 23,800 m^3/day. The total area of the survey that contained a volumetric gas flux greater than the threshold volumetric gas flux value is 0.86 km^2, which is 21% of the total surveyed area.

Although all focus seep sites demonstrate seep activity, the results shown in Figure 1 suggest that the seep activity is relatively diffuse throughout the La Goleta, Patch and Trilogy sites; while the seeps at Platform Holly and Seep Tent appear to be localized. For example, seep activity in the immediate vicinity of Platform Holly was concentrated on the west side of the platform and extended approximately 150 m to the west in a narrow band.

Table 1. Estimates of the maximum volumetric gas flux and the integrated volumetric gas flow rates, gridded in 25 m by 25 m cells, at standard temperature and pressure (0 °C and 101 kPa) in the Coal Oil Point seep field during 31 August 2016 to 14 September 2016 acoustic survey.

Seep Site	Survey Dates	Minimum Survey Location	Maximum Survey Location	Area Surveyed (km^2)	Area of Seepage Activity (km^2)	q_{max} ($m^3/m^2/day$)	Q_{total} (m^3/day)
Platform Holly	6 Sept 2016	34°22'20.45" N, 119°54'40.00" W	34°23'43.09" N, 119°54'20.17" W	0.367	0.034	0.75	1,490
Seep Tent	7 Sept 2016	34°22'54.64" N, 119°53'33.25" W	34°23'11.33" N, 119°53'10.46" W	0.338	0.051	0.19	990
La Goleta	7 Sept 2016	34°22'20.30" N, 119°51'22.04" W	34°22'38.16" N, 119°50'59.04" W	0.375	0.215	0.57	5,350
Patch	2 Sept 2016	34°21'40.87" N, 119°49'59.35" W	34°21'58.79" N, 119°49'33.62" W	0.366	0.203	0.13	4,220
Trilogy	8 Sept 2016	34°23'30.94" N, 119°53'01.57" W	34°23'51.53" N, 119°52'17.0" W	0.747	0.187	2.6	8,980

Visual observations during the survey confirmed surfacing gas bubbles and oil droplets near, and possibly under, the west side of the platform. Surfacing gas bubbles and surface slicks of oil were common throughout the region during the time of the survey. It is also worth noting that oil droplets in the water column were visually observed during BCD sampling (Figure 6) and have been observed in previous studies (Leifer et al., 2006). Estimates of oil droplet size were extracted from the video images acquired with the BCD, using the gradations on the cylinder for a length reference. The range of oil droplet size was approximately 0.7-5.4 mm in radius, where the lowest estimate of droplet size is limited to the resolution of the video camera mounted on the BCD.

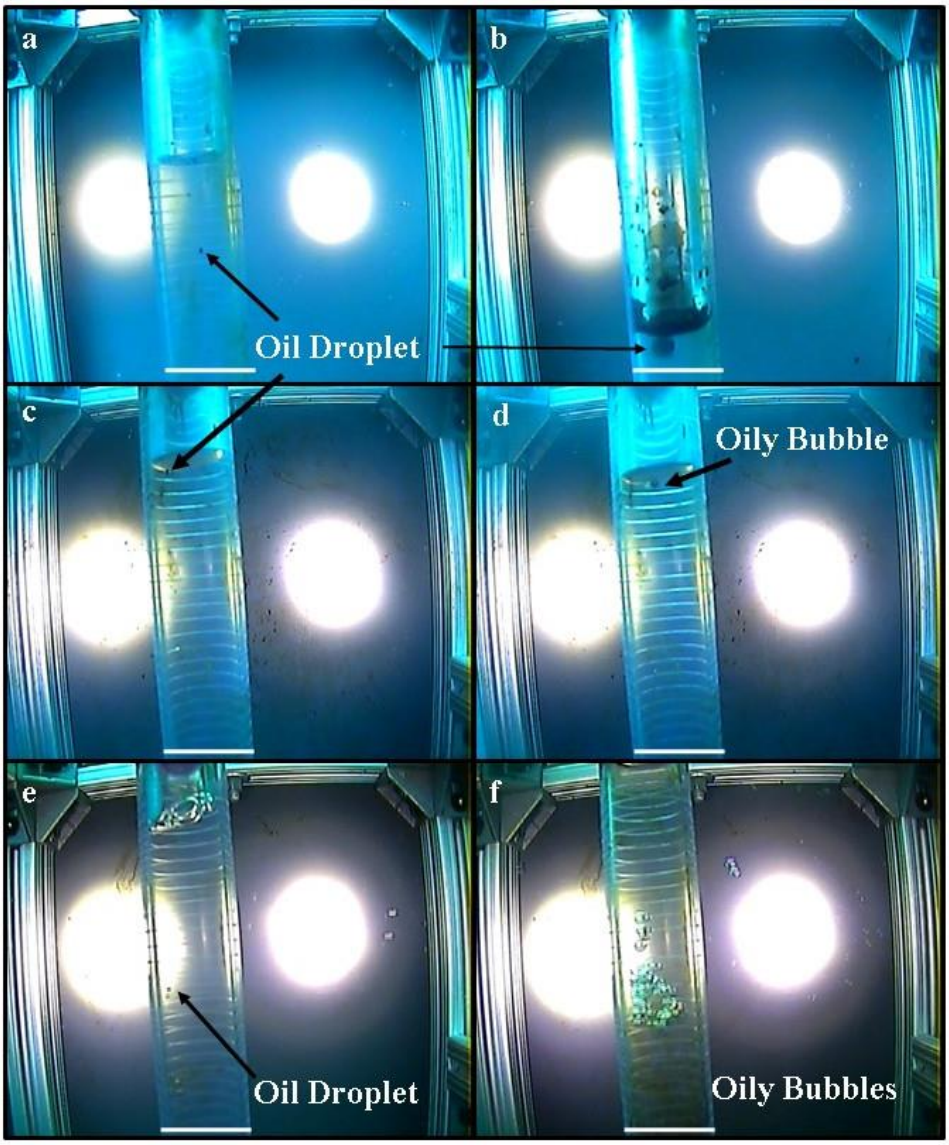

Figure 6. Images from the drop camera of oil droplets and gas bubbles in the BCD. Observations from Platform Holly (a, b), Seep Tent (c, d) and La Goleta (e, f). The red line is approximately 33 mm in length.

4 Comparison of Volumetric Gas Flux Observations to Previous Estimates

Where possible, estimates of volumetric gas flux and volumetric gas flow rates obtained from this study were compared with previous estimates of volumetric gas flux and volumetric gas flow rates from different studies (Table 2). These comparisons were done for specific seep sites and areas of seepage activity that the studies had in common. Two types of estimates are generally reported: total volumetric gas flow rates (Q_{total}) for individual focus seep sites (e.g., Platform Holly) and maximum observed volumetric gas flux (q_{max}) localized within a focus seep site. This comparison is limited by the differences in coverage at the different focus seep sites, and sometimes by the lack of resolution in published data, but still provides useful context for evaluating the present study.

Table 2. Maximum volumetric gas flux and integrated volumetric gas flow rate estimates, at standard temperature and pressure (0 °C and 101 kPa), for different seep sites and studies within the Coal Oil Point seep field.

Survey Site	Study	Date	q_{max} ($m^3/m^2/day$)	Q_{total} (m^3/day)
Platform Holly – 2 km Radius	Hornafius et al., 1999	1994 - 1995	-	~ 17,000[d]
	This Study	Sep 2016	075[a]	2,540
Platform Holly	This Study	6 Sep 2016	0.75[a]	1,490
		26 Oct 2017	4.8[b]	-
Seep Tent	This Study	7 Sep 2016	0.19[a]	990
		26 Oct 2017	1.8[b]	-
La Goleta	Hornafius et al., 1999	1994 - 1995	> 0.1	~ 14,400[c]
	Washburn et al., 2005	20 Jun 2003	8.1	1,900
	Clark et al., 2010	29 Aug 2002	7.1	1,249
		20 Jun 2003	8.1	800
		15 Sep 2005	6.2	787
	This Study	7 Sep 2016	0.57[a]	5,350
		26 Oct 2017	16.3[b]	-
Patch	Hornafius et al., 1999	1994 - 1995	0.05 - 0.1	~ 2,600[c]
	This Study	2 Sep 2016	0.13[a]	4,220
Trilogy	Hornafius et al., 1999	1994 - 1995	0.05 - 0.1	~ 13,800[c]
	Clark et al., 2010	19 Sep 2005	8.2	5,472
		20 Sep 2005	7.6	4,159
	This Study	8 Sep 2016	2.6[a]	8,980

[a] Volumetric gas flux values obtained from 25 m by 25 m gridded data at STP, shown in Figure 1.

[b] Volumetric gas flux values obtained from discrete *in situ* volumetric gas flux measurement from the BCD, at STP.

[c] Volumetric gas flow rate values were obtained by overlaying Figure 3 (Hornafius et al., 1999) over Figure 1 (this study) and comparing the common areas of seepage activity between the two studies; estimates of integrated volumetric gas flow rates reported here were calculated using the median values of volumetric gas flux reported in Figure 3 (Hornafius et al., 1999).

[d] Volumetric gas flow rates reported in Table 1 from Hornafius et al., (1999).

In addition to the total volumetric gas flow rates and maximum observed volumetric gas flux, Hornafius et al. (1999) also reported a value that was the integrated volumetric gas flow rate for a circular region with a 2 km radius, centered on Platform Holly, an area that would include both the Platform Holly and Seep Tent seep sites and a small portion of the broad survey of the present study. This reported volumetric gas flow rate is seven times higher than that observed from the same region surveyed during this study. The results of volumetric gas flow rates reported by Hornafius et al. (1999) are also higher by a factor of three and two at La Goleta and Trilogy, respectively. However, the total volumetric gas flow rate observed at Patch in this study is higher than the estimates presented in Hornafius et al. (1999) by approximately a factor of two. The total volumetric gas flow rate estimates from Washburn et al. (2005) and Clark et al. (2010), measurements obtained using the “Flux Buoy” developed by Washburn et al. (2001), ranged over a factor of approximately three to seven times lower for La Goleta and are approximately a factor of two lower at Trilogy compared to results of total volumetric gas flow rates obtained in this study.

The area of seepage activity of the individual seep sites surveyed by Hornafius et al. (1999) was estimated similarly to the calculation of volumetric gas flow rate measurements for their broad acoustic survey (see footnote c in Table 2). The observed areas of seepage activity by Hornafius et al. (1999) are higher by 23% and 30% at La Goleta and Trilogy, respectively, and 24% lower at Patch compared to the areas of seepage activity from this study. Areas associated with estimates of volumetric gas flux and volumetric gas flow rates from Washburn et al. (2005) and Clark et al. (2010) overlapped this study for La Goleta, Patch and Trilogy. However, the results reported by Washburn et al. (2005) and Clark et al. (2010) were locally constrained to small areas (480-5,380 m^2) of high flux activity.

The reported maximum localized volumetric gas flux estimates (q_{max} in Table 1 and 2) vary considerably from site to site and methodology employed (acoustic versus direct capture). The maximum volumetric gas flux values reported in this study are derived from both the acoustic data, which represents the average s_v values in a 25 m by 25 m grid cell and are more comparable to Hornafius et al. (1999), and the BCD, which represents a cross-sectional area on the order of 1 m^2 and are more comparable to the "Flux Buoy" reported by Washburn et al. (2005) and Clark et al. (2010). Localized volumetric gas flux estimates in the present study were highest at Platform Holly, La Goleta and Trilogy. Washburn et al. (2005) and Clark et al. (2010) reported very similar localized volumetric gas flux estimates at La Goleta and Trilogy. The localized volumetric gas flux estimates observed by Hornafius et al. (1999) were similar to those found in the present study at Patch, an order of magnitude lower at Trilogy, and were consistent but difficult to compare, due to figure resolution, for La Goleta.

The differences observed between the estimated volumetric gas flux and volumetric gas flow rate measurements from this study and the estimates reported in previous studies (Clark et al., 2010; Hornafius et al., 1999; Washburn et al., 2005) may be due to differences between the methodologies employed to obtain volumetric gas flux measurements. Hornafius et al. (1999) surveyed the Coal Oil Point seep field using a widebeam transducer (35° beam width) that was calibrated with a synthetic bubble plume source with a known volumetric gas flow rate in order to convert acoustic measurements to volumetric gas flow rates for the region. The method used in the present study differed from that of Hornafius et al. (1999) in two major ways: 1) a narrower (7° beam width) split-beam echosounder was used in this study, and 2) instead of using a synthetic plume, this study used the BCD to collect direct, *in situ* volumetric gas flux measurements from several Coal Oil Point seep sites in order to convert acoustic backscatter measurements into estimates of volumetric gas flux.

The spatial coverage obtained by Hornafius et al. (1999) and this study are dependent on the acoustic system used during the survey. The acoustic system used by Hornafius et al. (1999) had a 35° beam width, which at an investigation depth layer of 23 m yields an acoustic beam footprint diameter of 14 m. A 7° beam width split-beam echosounder was used in this study and the diameter of the acoustic beam footprint was 2.8 m at a water depth of 23 m. This means that for the dense survey lines conducted in this study, 10 m for the deep focus seep sites and 20 m for Trilogy, approximately 28% and 14% of the seep sites were mapped, respectively. As shown in Figure 4, estimates of S_v can vary between 20-25 dB over distances that are less than the line spacing used to survey the seep sites in this study. This variability in seepage intensity was also observed by Washburn et al. (2005) with the use of the "Flux Buoy". Therefore, even though dense survey lines were used in this study to map the seepage activity at each of the individual

seep sites, 72-86 % of the spatial distribution was not mapped due to the narrow beam width of the acoustic system used throughout the survey. Since there is no information about the line spacing used by Hornafius et al. (1999) during their acoustic survey, it is difficult to compare the spatial coverage between this study and Hornafius et al. (1999). Incomplete spatial coverage is a limitation for many direct measurement instruments (i.e., "Flux Buoy" and BCD) and for narrow beam acoustic transducers due to their small cross-sectional area or small beam widths, respectively. Recent studies on gas flow in the ocean have attempted to address the limited coverage in acoustic surveys by using multibeam echosounders, which can cover large spatial areas compared to narrow beam echosounders and direct measurement devices (Römer et al. 2017).

The second major difference between Hornafius et al. (1999) and this study is the approach used in order to convert s_v into estimates of volumetric gas flux. The use of synthetic plumes can lead to bias in the estimate of volumetric gas flux because the unknown bubble size distribution of the synthetic plume likely differs from that of the natural seep. An attempt was made to avoid this bias in the present study by calibrating the acoustic measurements with direct volumetric gas flux estimates, using the BCD, at seep sites within the Coal Oil Point seep field. Measurements of direct volumetric gas flux, in tandem with s_v measurements, were obtained for three of the five focus seep sites (i.e., Platform Holly, Seep Tent and La Goleta) and were collected at regions of high seepage activity. It is assumed that the bubble size distribution and the relationship between s_v and volumetric gas flux obtained at these three seep sites can be extrapolated to the entire survey.

At Seep Tent and La Goleta, measurements of volumetric gas flux from the BCD were obtained at a depth of 23 m in order to be consistent with the average depth layer used in previous studies (i.e., Hornafius et al., 1999). However, in the vicinity of Platform Holly, the depth layer was reduced to 15 m due to safety concerns related to the proximity of the platform to the BCD and vessel. This change in direct volumetric gas flux measurement depths with the BCD may have caused a change in bubble size distribution, leading to a bias in volumetric gas flux estimates. The potential changes in bubble sizes are caused by a combination of gas transfer through the gas-liquid interface and changes in hydrostatic pressure as gas bubbles rise through the water column (McGinnis et al., 2006; Rehder et al., 2009). In order to assess the relevance of these changes, the Texas A&M Oilspill Calculator (TAMOC) model (Gros et al., 2016; Gros et al., 2017) was used to predict the changes in bubble size as a function of depth. The TAMOC model was provided with bubble gas composition at a depth of 70 m (see supporting information, Table S2), aqueous concentration of oxygen (Scripps Institution of Oceanography, 2017; see supporting information, Table S1) and atmospheric equilibrium nitrogen concentration. The results from the TAMOC model (see supporting information) show that the bubble size changes by approximately 1-7 % over a change in water depth from 23 m to 15 m for bubble sizes between 1-5 mm in radius. The TAMOC models also show that although the gas bubble size is relatively unchanging during their ascent though the water column, the gas composition within the bubble changes substantially. For larger bubbles, with radii greater than 3.5 mm, the gas composition of methane in the bubble changes from 82% at the seabed to approximately 70% at 23 m. For a 3.5 mm radius bubble, the mass of methane inside the bubble changes from 8.1×10^{-4} g to 1.5×10^{-4} g. Due to the fact that a gas bubble's radius does not change dramatically during ascent through the water column, estimates of volumetric gas flux and volumetric gas flow rates are not affected by bubble dissolution, only gas composition within the bubble is affected by

dissolution. However, the estimates of volumetric gas flux and volumetric gas flow rates in this study are reported at STP, in order to compare with results from previous studies, which does not take into consideration the mass transfer of gas between the bubble and the surrounding water column. Therefore, if it is desired to estimate the molar gas flux/flow at the sea surface or the amount of methane that survives from the water column into the atmosphere, mass transfer across the gas-liquid boundary must be taken into account.

The presence of oil, in the form of surface oil slicks and rising oil droplets, was visually observed throughout the entire 2016 acoustic survey. Oil droplets were also collected during the BCD volumetric gas flux measurements (shown in Figure 6), however only near the vicinity of Platform Holly was there a high concentration of oil droplets to cause a layer of oil to form between the gas-water interface. This accumulation of oil near Platform Holly was not included in the volumetric gas flux measurements obtained with the BCD and was still considered to be a negligible contribution to the integrated volumetric gas flow rate results. In order to have a non-negligible contribution to estimates of volumetric gas flow rates, there would need to be a higher concentration of oil droplets within the surrounding gas bubbles. For example, when observing the target strength (the decibel equivalent of the acoustic backscattering cross-section, σ_{bs}) of oil droplets and gas bubbles over the frequency range used in this study, at least twenty-five 2.5 mm radius oil droplets are needed in order to see a deviation of approximately 1 dB in the target strength of a single 2.5 mm radius gas bubble. This corresponds to a factor of 25 volumetric ratio of oil droplets to gas bubbles, which was not observed to occur during this study.

There is a high degree of variability in volumetric gas flow rates, both between investigators and the different methods used in each individual study, and for sites visited multiple times (e.g., Clark et al. (2010) visited La Goleta in 2002, 2003 and 2005). This variability is consistent with other studies for which seep activity has been observed to vary over timescales of seconds to minutes and hours to years (Boles et al., 2001; Clark et al., 2003; Clark et al., 2010; Hornafius et al., 1999; Jerram et al., 2015; Kinnaman et al., 2010; Leifer and Boles, 2005; Quigley et al., 1999). Quigley et al. (1999) reported a decrease of seep activity of 80% in the vicinity of Platform Holly in a 22-year period, by comparing the area of detected seeps (but not volumetric gas flow rates) to those of Fischer and Stevenson (1973), and that reduction has been hypothesized to be linked to petroleum extraction from Platform Holly. This reduction is consistent with the reduction found in the present study when compared to the results reported by Hornafius et al. (1999) over a 21-year period. However, Hornafius et al. (1999) also show a larger volumetric gas flow rate, by a factor of three, than the present study at La Goleta, a region sufficiently removed from Platform Holly that reservoir connectivity is highly unlikely; Hornafius et al. (1999) also present a volumetric gas flow rate estimate lower than the estimate obtained in this study at Patch. Hornafius et al. (1999) estimated that the volumetric gas flow rate over an 18 km^2 acoustic survey in the Coal Oil Point seep field was approximately 1.48 x 10^3 m^3/day, which does not include the gas captured by the containment tent located in Seep Tent. A comparison of the total volumetric gas flow rate estimate between this study and Hornafius et al. (1999) is difficult to assess due to differences in the surveyed areas. The surveyed area from Hornafius et al. (1999) is approximately 4 times larger than the area surveyed in this study and the area that exhibited seepage activity is 14 times lower in this study compared to the 12.5 km^2 of seepage activity reported in 1999. In addition, the methodologies used by this study and Hornafius et al. (1999) to estimate volumetric gas flow rates in the Coal Oil Point seep field are different. The differences in volumetric gas flow rate estimates from this study and previous

484 studies (Clark et al., 2010; Hornafius et al., 1999; Washburn et al., 2005) can also be caused by
485 uncertainties related to low spatial coverage of seepage activity in the seep field. Therefore,
486 similar uncertainties in estimates of volumetric gas flow rates could have been observed, due to
487 low spatial coverage, even if all studies had used the same approach for obtaining measurements
488 of volumetric gas flow rates. Thus, it is difficult to discriminate whether the differences in
489 volumetric gas flow rates in the seep field are attributed to the natural variability of the seep site
490 or if it is caused by the different approaches used in order to estimate the volumetric gas flow
491 rate in the region.

492 **5 Conclusions**

493 In this study, a portion of the current spatial distribution of seeps within the Coal Oil Point seep
494 field was mapped, and the integrated volumetric gas flow rate was estimated at four "deep" focus
495 seep sites (Platform Holly, Seep Tent, La Goleta and Patch) and at one "shallow" focus seep site
496 (Trilogy). The estimated total volumetric gas flow rate from the acoustic survey was 23,800
497 m^3/day over a total surveyed area of 4.1 km^2. Of the deep focus seep sites, La Goleta and
498 Platform Holly demonstrated the most vigorous gas seeps. Oil droplets were visually observed at
499 Platform Holly, Seep Tent and La Goleta and ranged in radius from approximately 0.7-5.4 mm.

500 Comparisons of integrated volumetric gas flow rates at individual seep sites within the Coal Oil
501 Point seep field were made between the new estimates obtained from this study and those
502 reported in previous studies. The broad acoustic survey in the Coal Oil Point seep field
503 conducted in this study shows that the seep field is still active, however, volumetric gas flow
504 rates, at specific seep sites, range from two to seven times smaller than estimates obtained by
505 Hornafius et al. (1999) between the years 1994-1995. Given the variability in results and in
506 methodologies used in order to obtain estimates of volumetric gas flow rates within the seep
507 field, it is difficult to assess changes in volumetric gas flow rates for the Coal Oil Point seep
508 field, or at focus seep sites within the region. Current methods, such as acoustic instruments
509 and/or direct measurement devices, used to obtain estimates of volumetric gas flow rates still
510 have large uncertainties. Therefore, developing reliable techniques in tandem with establishing a
511 consistent and accurate methodology to calculate volumetric gas flow rates within the Coal Oil
512 Point seep field will prevent methodological bias and potentially help understand how volumetric
513 gas flow rates are affected by natural variability within the seep field as well as anthropogenic
514 processes.

515 **Acknowledgments, Samples, and Data**

516 This work was supported under the BSEE Cooperative Agreement Award No. E16AC00002, and
517 NSF Grants 1352301 and 1756947. The first author would also like to acknowledge the NSF
518 Graduate Research Fellowship Program for support. We would like to acknowledge and thank
519 the crew of the *R/V Connell*, Christoph Pierre and Christian Orsini for piloting the vessel and
520 their patience throughout the entire survey. We would also like to acknowledge Josh Inga and
521 Nancy Torres (UCSB) for their participation in the acoustic survey and Michelle Domino (UNH)
522 for processing BCD video images. Data collected during the 2016 and 2017 surveys are available
523 at the NOAA National Center for Environmental Information repository at
524 http://doi.org/10.25921/3x3w-qf48 and http://doi.org/10.25921/1q3m-3689, respectively.

References

Anderson, V. C. (1950), Sound scattering from a fluid sphere. *The Journal of the Acoustical Society of America*, 22(4), 426-431. https://doi.org/10.1121/1.1906621

Boles, J. R., Clark, J. F., Leifer, I., & Washburn, L. (2001), Temporal variation in natural methane seep rate due to tides, Coal Oil Point area, California. *Journal of Geophysical Research*, 106 (11), 27077-20786. https://doi.org/10.1029/2000JC000774

Boles, J. R., Eichhubl, P., Garven, G., & Chen, J. (2004), Evolution of a hydrocarbon migration pathway along basin-bounding faults: Evidence from fault cement. *AAPG bulletin*, 88 (7), 947-970. https://doi.org/10.1306/02090403040

Clark, J. F., Leifer, I., Washburn, L., & Luyendyk, B. P. (2003), Compositional changes in natural gas bubble plumes: observations from the Coal Oil Point marine hydrocarbon seep field. *Geo-Marine Letters*, 23 (3-4), 187-193. https://doi.org/10.1007/s00367-003-0137-y

Clark, J. F., Washburn, L., & Schwager Emery, K. (2010), Variability of gas composition and flux intensity in natural marine hydrocarbon seeps. *Geo-Marine Letters*, 30, 379-388. https://doi.org/10.1007/s00367-009-0167-1

Clay, C. S. & Medwin, H. (1977), *Acoustical oceanography: principles and applications*, pp. 194-210, New York: John Wiley & Sons.

Demer, D. A., Berger, L., Bernasconi, M., Bethke, E., Boswell, K., Chu., D, et al. (2015), Calibration of acoustic instruments. *ICES Cooperative Research Report*, 326, 1-133.

Fischer, P. J., & Stevenson, A. J. (1973), Natural hydrocarbon seeps along the northern shelf of the Santa Barbara Basin. *Santa Barbara Channel Region Revisited*, pp. 17-28, Tulsa, Oklahoma: American Association of Petroleum Geology.

Francois, R. E., & Garrison, G. R. (1982), Sound absorption based on ocean measurements: Part I: Pure water and magnesium sulfate contributions. *The Journal of the Acoustical Society of America*, 72 (3), 896-907. https://doi.org/10.1121/1.388170

Greinert, J., Artemov, Y., Egorov, V., De Batist, M., & McGinnis, D. (2006), 1300-m-high rising bubbles from mud volcanoes at 2080 m in the Black Sea: Hydroacoustic characteristics and temporal variability. *Earth and Planetary Science Letters*, 244 (1-2), 1-15. https://doi.org/10.1016/j.epsl.2006.02.011

Greinert, J., McGinnis, D. F., Naudts, L., Linke, P., & De Batist, M. (2010), Atmospheric methane flux from bubbling seeps: Spatially extrapolated quantification from a Black Sea shelf area. *Journal of Geophysical Research: Oceans*, 115 (C1), 1-18. https://doi.org/10.1029/2009JC005381

Gros, J., Reddy, C. M., Nelson, R. K, Socolofsky, S. A., & Arey, J. S. (2016), Simulating gas-liquid water partitioning and fluid particles of petroleum under pressure: implications for deep-

560 sea blowouts. *Environmental Science and Technology*, 50 (14), 7397-7408.
561 https://doi.org/10.1021/acs.est.5b04617

562 Gros, J., Socolofsky, S. A., Dissanayake, A. L., Jun, I., Zhao, L., Boufadel, M. C., et al. (2017),
563 Petroleum dynamics in the sea and influence of subsea dispersant injection during Deepwater
564 Horizon. *Proceedings of the National Academy of Sciences,* 114 (38), 10065-10070.
565 https://doi.org/10.1073/pnas.1612518114

566 Heeschen, K. U., Tréhu, A. M., Collier, R. W., Suess, E., & Rehder, G. (2003), Distribution and
567 height of methane bubble plumes on the Cascadia Margin characterized by acoustic imaging.
568 *Geophysical Research Letters*, 30 (12), 1-4. https://doi.org/10.1029/2003GL016974

569 Hill, T. M., Kennett, J. P., Valentine, D. L., Yang, Z., Reddy, C. M., Nelson, R. K., et al. (2006),
570 Climatically driven emissions of hydrocarbons from marine sediments during deglaciation.
571 *Proceedings of the National Academy of Science*, 103 (37), 13570-13574.
572 https://doi.org/10.1073/pnas.0601304103

573 Hornafius, J. S., Quigley, D., & Luyendyk, B. P. (1999), The world's most spectacular marine
574 hydrocarbon seeps (Coal Oil Point, Santa Barbara Channel, California): Quantification of
575 emissions. *Journal of Geophysical Research*, 104 (9), 20703-20711.
576 https://doi.org/10.1029/1999JC900148

577 Hovland, M., & Judd, A. G. (1992), The global production of methane from shallow submarine
578 sources. *Continental Shelf Research*, 12 (10), 1231-1238. https://doi.org/10.1016/0278-
579 4343(92)90082-U

580 Jerram, K., Weber, T. C., & Beaudoin, J. (2015), Split-beam echo sounder observation of natural
581 methane seep variability in the northern Gulf of Mexico. *Geochemistry, Geophysics,*
582 *Geosystems*, 16, 736-750. https://doi.org/10.1002/2014GC005429

583 Kinnaman, F. S., Kimball, J. B., Busso, L., Birgel, D., Ding, H., Hinrichs, K. U., & Valentine, D.
584 L. (2010), Gas flux and carbonate occurrence at a shallow seep of thermogenic natural gas. *Geo-*
585 *Marine Letters*, 30 (3-4), 355-365. https://doi.org/10.1007/s00367-010-0184-0

586 Leifer, I., & Boles, J. (2005), Turbine tent measurements of marine hydrocarbon seeps on
587 subhourly timescales. *Journal of Geophysical Research*, 110, 1-12.
588 https://doi.org/10.1029/2003JC002207

589 Leifer, I., Clark, J. F., & Chen, R. F. (2000), Modifications of the local environment by natural
590 marine hydrocarbon seeps. *Geophysical Research Letters*, 27 (22), 3711-3714.
591 https://doi.org/10.1029/2000GL011619

592 Leifer, I., Kamerling, M. J., Luyendyk, B. P., & Wilson, D. S. (2010), Geologic control of
593 natural marine hydrocarbon seep emissions, Coal Oil Point seep field, California. *Geo-Marine*
594 *Letters*, 30 (3-4), 331-338. https://doi.org/10.1007/s00367-010-0188-9

595 Leifer, I., Luyendyk, B. P., & Broderick, K. (2006), Tracking oil slick from multiple natural
596 sources, Coal Oil Point, California. *Marine and Petroleum Geology*, 23, 621-630.
597 https//doi.org/10.1016/j.marpetgeo.2006.05.001

598 Loranger, S., Bassett, C., Cole, J. P., Boyle, B., & Weber, T. C. (2018), Acoustically relevant
599 properties of four crude oils at oceanographic temperatures and pressures. *The Journal of the*
600 *Acoustical Society of America*, 144 (5), 2926-2936. https://doi.org/10.1121/1.5078606

601 MacLennan, D. N., Fernandes, P. G., & Dalen, J. (2002), A consistent approach to definitions
602 and symbol in fisheries acoustics. *ICES Journal of Marine Science*, 59 (2), 365-369.
603 https://doi.org/10.1006/jmsc.2001.1158

604 Mau, S., Valentine, D. L., Clark, J. F., Reed, J., Camilli, R., & Washburn, L. (2007), Dissolved
605 methane distributions and air-sea flux in the plume of a massive seep field, Coal Oil Point,
606 California. *Geophysical Research Letters*, 34 (22), 1-5. https://doi.org/10.1029/2007GL031344

607 Medwin, H., & Breitz, N. D. (1989), Ambient and transient bubble spectral densities in quiescent
608 seas and under spilling breaker. *Journal of Geophysical Research: Oceans*, 94 (C4), 12751-
609 12759. https://doi.org/10.1029/JC094iC09p12751

610 McGinnis, D. F., Greinert, J., Artemov, Y., Beaubien, S. E., Wüest, A. (2006), Fate of rising
611 methane bubbles in stratified waters: How much methane reaches the atmosphere? *Journal of*
612 *Geophysical Research: Oceans*, 11 (C9), 1-15. https://doi.org/10.1029/2005JC003183

613 Nikolovska, A., Sahling, H., & Bohrmann, G. (2008), Hydroacoustic methodology for detection,
614 localization, and quantification of gas bubbles rising from the seafloor at gas seeps from the
615 eastern Black Sea. *Geochemistry, Geophysics, Geosystems*, 9 (10), 1-13.
616 https://doi.org/10.1029/2008GC002118

617 Quigley, D. C., Hornafius, J. S., Luyendyk, B. P., Francis, R. D., Clark, J., & Washburn, L.
618 (1999), Decrease in natural marine hydrocarbon seepage near Coal Oil Point, California,
619 associated with offshore oil production. *Geology*, 27 (11), 1047-1050.
620 https://doi.org/10.1130/0091-7613(1999)027<1047:DINMHS>2.3.CO;2

621 Rehder, G., Leifer, I., Brewer, P.G., Friederich, G., Peltzer, E.T. (2009), Controls on methane
622 bubble dissolution inside and outside the hydrate stability field from open ocean field
623 experiments and numerical modeling. *Marine Chemistry*, 114, 19–30.
624 https://doi.org/10.1016/j.marchem.2009.03.004

625 Römer, M., Sahling, H., Pape, T., Bahr, A., Feseker, T., Wintersteller, P, et al. (2012a),
626 Geological control and magnitude of methane ebullition from a high-flux seep area in the Black
627 Sea – the Kerch seep area. *Marine Geology*, 391, 57-74.
628 https://doi.org/10.1016/j.margeo.2012.07.005

629 Römer, M., Sahling, H., Pape, T., Bohrmann, G., & Speiß, V. (2012b), Quantification of gas
630 bubble emissions from submarine hydrocarbon seeps at the Makran continental margin (offshore
631 Pakistan). *Journal of Geophysical Research: Oceans*, 117 (C10), 1-
632 19.https://doi.org/10.1029/2011JC007424

Römer, M., Wenau, S., Mau, S., Veloso, M., Greinert, J., Schlüter, M., et al. (2017), Assessing marine gas emission activity and contribution to the atmospheric methane inventory: A multidisciplinary approach from the Dutch Dogger Bank seep area (North Sea). *Geochemistry, Geophysics, Geosystems*, 18, 2617–2633. https://doi.org/10.1002/2017GC006995

Scripps Institution of Oceanography, University of California (2017), *Physical, Chemical and Biological Data, CalCOFI Cruise 1607*. CC Ref. 17-03, 1-54. http://calcofi.org/data/data_reports/2016/1607final.pdf

Terrill, E. J., & Melville, W. K. (2000), A broadband acoustic technique for measuring bubble size distributions: Laboratory and shallow water measurements. *Journal of Atmospheric and Ocean Technology*, 17 (2), 220-239. https://doi.org/10.1175/1520-0426(2000)017<0220:ABATFM>2.0.CO;2

Vagle, S., & Farmer, D. M. (1992), The measurement of bubble-size distributions by acoustic backscatter. *Journal of Atmospheric and Oceanic Technology*, 9 (5), 630-644. https://doi.org/10.1175/1520-0426(1992)009<0630:TMOBSD>2.0.CO;2

Valentine, D. L., Reddy, C. M., Farwell, C., Hill, T. M., Pizarro, O., Yoerger, D. R., et al. (2010), Asphalt volcanoes as a potential source of methane to late Pleistocene coastal waters. *Nature Geosciences*, 3 (5), 345-348. https://doi.org/10.1038/ngeo848

Washburn, L., Clark, J. F., & Kyriakidis, P. (2005), The spatial scales, distribution, and intensity of natural marine hydrocarbon seeps near Coal Oil Point, California. *Marine and Petroleum Geology*, 22 (4), 569-578. https://doi.org/10.1016/j.marpetgeo.2004.08.006

Washburn, L., Johnson, C., Gotschalk, C. C., & Egland, E. T. (2001), A gas-capture buoy for measuring bubbling gas flux in ocean and lakes. *Journal of Atmospheric and Oceanic Technology*, 18 (8), 1411-1420. https://doi.org/10.1175/1520-0426(2001)018<1411:AGCBFM>2.0.CO;2

Wang, B., Socolofsky, S. A., Breier, J. A., & Seewald, J. S. (2016), Observations of bubbles in natural seep flares at MC 118 and GC 600 using in situ quantitative imaging. *Journal of Geophysical Research: Oceans*, 121 (4), 2203-2230. https://doi.org/10.1002/2015JC011452

Weber, T. C., De Robertis, A., Greenaway, S. F., Smith, S., Mayer, L., & Rice, G. (2012), Estimating oil concentration and flow rate with calibrated vessel-mounter acoustic echo sounder. *Proceedings of the National Academy of Sciences*, 109 (50), 20240-20245. https://doi.org/10.1073/pnas.1108771108

Weber, T. C., Mayer, L., Jerram, K., Beaudoin, J., Rzhanov, Y., & Lovalvo, D. (2014), Acoustic estimates of methane gas flux from the seabed in a 6000 km^2 region in the Northern Gulf of Mexico. *Geochemistry, Geophysics, Geosystems*, 15, 1911-1925. https://doi.org/10.1002/2014GC005271

Weber, T. C., & Ward, L. G. (2015), Observations of backscatter from sand and gravel seafloors between 170 and 250 kHz. *The Journal of the Acoustical Society of America*, 138 (4), 2169-2180. https://doi.org/10.1121/1.4930185